Neural-Network-Based Root Mean Delay Spread Model for Ubiquitous Indoor Internet-of-Things Scenarios

Yu Yu, Wen-Jun Lu, *Senior Member, IEEE*, Yang Liu, *Member, IEEE*, and Hong-Bo Zhu

***Abstract*—Massive robust communication demands among machines and humans are required in ubiquitous Internet-of-Things (IoT) applications. To design the appropriate communication system, the knowledge of the propagation characteristics for various IoTs scenarios is necessary. In this article, a measurement-based neural-network-based root-mean-square (RMS) delay spread model for ubiquitous indoor IoTs scenarios is presented. The proposed model is a two-layer feedforward neural network plus a random variable, characterizing the average RMS delay spread and uncertain shadowing effect, respectively. The neural network consists of five inputs, including transmitting/receiving antennas (Tx/Rx) separation, frequency, antenna height, environment, and line-of-sight/non-line-of-sight (LOS/NLOS) propagation condition, seven hidden layer neurons, and one output layer neuron. Compared with different configurations of the neural network, the hyperbolic tangent sigmoid functions and the Levenberg–Marquardt backpropagation algorithm are selected as neurons' activation functions and training method, respectively. Additionally, the random variable is found to follow the normal distribution using the maximum-likelihood estimation. Finally, the novel model is experimentally validated to be accurate, general, and extensible compared with the conventional normally distributed RMS delay spread model. This model is well applicable to the design and planning of the ubiquitous communication links for future IoTs scenarios.**

***Index Terms*—Internet of Things (IoT), neural network, root mean-square (RMS) delay spread, shadowing.**

I. Introduction

THE APPLICATION of the Internet of Things (IoT) is considered to be a significant feature in current and future wireless communication systems [1], [2]. With the emergence of ubiquitous IoTs scenarios, i.e., smart home, smart building, smart grid, smart transportation, etc., massive smart devices and sensors are distributed in the environments [3]–[5]. A large amount of communication links among these machines and users should be established [6]. Actually, communication links must meet the requirements of stability, throughput, and latency in IoTs applications [7], [8]. In order to ensure such communication requirements, the comprehensive knowledge of the characteristics of the indoor environments is important for the design of the communication systems and the deployment of the smart devices and sensors [9], [10].

The root-mean-square (RMS) delay spread characterizes the severity of the multipath fading and time dispersion [11], [12]. It is a crucial metric of the propagation properties, directly affecting the design of the multiplexing methods, the digital modulations, and the signal waveforms [13]. Although the communication distance in indoor environments is small compared with the one of outdoor environments, the multipath fading for indoor communication is still serious since the various scenarios, rich scatters, and complex structures, especially at the low-frequency band. Thus, the modeling of the RMS delay spread property in indoor environments is a problem needed to be solved. Recently, the RMS delay spreads of indoor environments have been extensively investigated [14]–[17]. For example, its statistical properties and distributions in different indoor environments, propagation conditions, and frequencies have been summarized in [18]. In [19], the RMS delay spread has been found to follow normal distributions and its dependency on the distance and path loss has been studied. The antenna height and polarization effects on RMS delay spread have been studied in [20] and [21]. More recently, a lognormally distributed RMS delay spread model of the massive MIMO channel at 11 GHz has been proposed [22]. However, these works share three commonalities: 1) the existing models are proposed based on measured data over a large distance range; 2) the quantitative relationships among the RMS delay spread and some important inputs are seldom researched; and 3) the generality and extendibility of these models are not fully considered. Actually, an alternative solution to satisfy the communication requirements in IoTs scenarios is to offload part of the communication and computing tasks to the edge of the networks [23], [24]. In this case, many IoTs scenarios may happen in complex indoor environments with scattered and deep multipath fading propagation characteristics, e.g., rooms, offices, stairs, corridors, etc. The indoor short-range communication will become the main type of communication among the machines and the users [25], [26]. Additionally, the environments, frequencies,

Manuscript received November 24, 2019; revised February 14, 2020; accepted March 6, 2020. Date of publication March 10, 2020; date of current version June 12, 2020. This work was supported by the High-Level Research Initiation Foundation for Introduction of Talents of Nanjing Institute of Technology under Grant YKJ201970. *(Corresponding author: Yu Yu.)*

Yu Yu is with the School of Information and Communication Engineering, Nanjing Institute of Technology, Nanjing 211167, China (e-mail: yuyu@njit.edu.cn).

Wen-Jun Lu and Hong-Bo Zhu are with the Jiangsu Key Laboratory of Wireless Communications, Nanjing University of Posts and Telecommunications, Nanjing 210003, China.

Yang Liu is with the Jiangsu Provincial Engineering Laboratory of Pattern Recognition and Computational Intelligence, Jiangnan University, Wuxi 214122, China.

Digital Object Identifier 10.1109/JIOT.2020.2979766

users' postures, sensors' positions/heights, smart devices' statuses, and other factors may be different in various IoTs applications [27]–[29]. To quantitatively describe these effects, more inputs need to be considered. Therefore, the correction terms should be introduced into the existing models such as the normal random variable RMS delay spread model [18]. However, the expressions of the correction terms are unknown and should be experimentally modeled or theoretically proved. Thus, the effectiveness and generality of the existing models will be limited when employed to the ubiquitous indoor IoTs scenarios.

Therefore, extensive channel measurements should be conducted in typical indoor environments of office buildings, i.e., office, corridor, and stair. They correspond to different scenarios for IoTs applications, such as smart office [27], fire alarm/rescue [30], intelligent monitoring [31], etc. In addition, the neural network cloud be adopted to improve the generality and expansibility of the model. As a branch of machine learning, the neural network shows high accuracy and good generality in solving the fitting problem. It has been applied to several areas of electromagnetic, antenna, and propagation [32]–[34]. The recent works about the neural network-based propagation models are summarized in the Table I [35]–[43]. The path losses for line-of-sight (LOS) and non-line-of-sight (NLOS) conditions have been modeled by a single and hybrid neural networks, respectively, [35]. The UWB channel path loss can be well represented by a neural network based on multilayer perceptron [36]. In [37], a heuristic model has been proposed by combining the neural network prediction approach with the multiple regression to describe the path loss in different residence environments. The neural network-based path loss model has been found to be more precise than the Hata model based on extensive outdoor measurements [38]. The relationship between the frequency and channel frequency response has been modeled using feedforward and radial basis function neural networks [39]. The performances of three dynamic neural networks, namely, focused time-delay neural network, distributed time-delay neural network, and layer recurrent neural network when they are applied to describe the path loss have been evaluated in [40]. Both of the artificial neural network and other machine learning methods, i.e., adaptive neural fuzzy inference system [41] and random forests [42], have been used for modeling the path loss. The effects of input parameters, the number of hidden neurons, activation functions, and learning algorithms on the accuracy of the neural network-based path loss model have been investigated [43].

Nevertheless, it is hard to directly apply these models to predict the RMS delay spread in IoTs scenarios for the following reasons: 1) most of the works focus on the prediction of the path loss rather than the RMS delay spread [35]–[38], [40]–[43]; 2) the shadowing effects describing the uncertainty of the RMS delay spread are rarely investigated; 3) the influences of the frequency, antenna height, environment, and propagation condition which are important for indoor channels are not considered [37], [43]; and 4) most of the channel sounding campaigns are carried out in the outdoor environments [35], [38], [40]–[43].

The RMS delay spread can provide useful information for the communication system design, such as the cyclic prefix length in the orthogonal frequency-division multiplexing (OFDM) system, the channel equalizer, the RAKE receiver, etc. [9], [12]. Especially, in various IoTs scenarios, the system designers need an accurate RMS delay spread model with diverse inputs to conveniently and fast determine the channel conditions. Motivated by the above challenges and the ubiquitous communication demands for IoTs scenarios, a novel measurement-based short-range RMS delay spread model with robustness, generality, and expansibility is essentially necessary and desirable [44]. Thus, measurement campaigns in three typical indoor environments, i.e., office, corridor, and stair are carried out at first. Then, a neural network-based RMS delay spread model is experimentally proposed. The main contributions of this article can be summarized as follows.

1) A novel RMS delay spread model combining the artificial neural network and random variable is proposed: The proposed model is a neural network plus a random variable, describing the certain and uncertain parts of the RMS delay spread, respectively. The advantages of the proposed model under this framework are accurate, general, and extensible.
2) More important inputs are included in the RMS delay spread model: Thanks to the neural network in the above model, the inputs related to the IoTs scenarios, including transmitting/receiving antennas (Tx/Rx) separation, frequencies, antenna height, environments, and LOS/NLOS propagation conditions, are introduced into the proposed model.
3) The shadowing effect of the RMS delay spread is researched for the first time: In the proposed model, the normal random variable is used for characterizing the uncertain shadowing effects of RMS delay spread. It can describe the phenomenon that the measured RMS delay spreads scatter around the fitted curves.
4) The impacts of different configurations of the neural network on the model accuracy are investigated: The effects of the key configurations of the neural networks, i.e., the activation functions of the neurons in the hidden layer and output layer, the training method, and weight/bias learning functions, on the accuracy of the model are studied. The best configuration is selected for extracting the parameters of the proposed model.

The remainder of this article is organized as follows. First, the experimental environments, measurement procedure, measurement system, and data extraction are performed in Section II. In Section III, the framework of the proposed neural network-based model is elaborately discussed. The effects of different configurations of the neural network on the model accuracy are investigated. Moreover, the validity of the proposed model is experimentally verified. Finally, in Section IV, the conclusion is drawn.

II. Measurement Settings

A. Experimental Environment and Measurement Procedure

The data used for modeling and validation are measured in three typical indoor environments (i.e., office, corridor,

(a) (b) (c)

Fig. 1. Photographs of measured environments: (a) office, (b) corridor, and (c) stair.

TABLE I
RECENT WORKS ABOUT PROPAGATION MODELING BASED ON NEURAL NETWORKS

Reference	Frequency	Environment	Input	Output
[35]	1890MHz	Outdoor	distance street width building height building separation Tx position	Path loss
[36]	3GHz-10GHz	Under Mine	distance frequency	Path loss
[37]	677MHz	Residence	distance residence type	Path loss
[38]	900MHz/ 1800MHz/ 100MHz	Outdoor	distance	Path loss
[39]	3GHz-11GHz/ 55GHz-65GHz	In-car	frequency Tx location Rx location	Channel frequency response
[40]	900MHz	Outdoor	distance Tx height Rx height	Path loss
[41]	1.8GHz	Outdoor	correction factor distance	Path loss
[42]	900MHz/ 1800MHz	Outdoor	building heights existence of streets LOS path	Path loss
[43]	189.25 MHz/ 479.25 MHz	Outdoor	distance longitude latitude elevation	Path loss

TABLE II
INFORMATION ABOUT MEASURED DATA USED FOR MODELING

Mark	Center Frequency	Environment	Usage	Measured Data Set
S1	2.595GHz	Office	Modeling	10 Rx heights 30 Rx points/height 9 grids/point 10 samples/grid total: 27000 samples
S2	2.595GHz	Corridor	Modeling	10 Rx heights 20 Rx points/height 9 grids/point 10 samples/grid total: 18000 samples
S3	2.595GHz	Stair	Modeling	10 Rx heights 23 Rx points/height 5 grids/point 10 samples/grid total: 11500 samples
S4	5.8GHz	Office	Modeling	10 Rx heights 30 Rx points/height 9 grids/point 10 samples/grid total: 27000 samples
S5	7.25GHz	Office	Modeling	10 Rx heights 30 Rx points/height 9 grids/point 10 samples/grid total: 27000 samples

and stair). The plan view of the measured environments and the deployment of the measured points are described elaborately in [45]. Fig. 1 shows the photographs of these environments. The detailed information about the measured environments, center frequencies, and data sets for channel modeling is tabulated in Table II. The size of the office is about 10.8 m × 7.5 m × 3.5 m (length × width × height). It consists of concrete walls, wooden doors, gypsum ceilings, and tiled floors. There are some desks, computers, electronic equipments, cabinet, and glass window in the office. The sizes of the T-shaped corridor and the indoor enclosed stair are about 15 m × 3.6 m × 3.8 m and 6.9 m × 3.5 m × 5.2 m, respectively. The materials of their walls, doors, ceilings, and floors are concrete, wooden, gypsum, and tiled, respectively. Additionally, there is a metal elevator in the corridor environment and wooden armrests in the stair environment.

The heights of the Tx antenna are 2.0 m, meanwhile, the heights of Rx change from 1 to 1.9 m with an interval of 0.1 m. At each Rx point, measurement grid points are employed. Moreover, ten frequency responses are recorded at each grid point for noise reduction [45]. With the variation of the Rx height and the location, both of the LOS and NLOS conditions are measured. During the measurements, the surroundings of the measured environment are frozen, therefore, the channel can be regarded as quasistatic.

It is worth noting that the collected data sets (S1–S5) in Table II are used for channel modeling and parameters extracting in Sections III-A and III-B. Additional measurements are carried out in the other two offices, corridor and stair environments with similar structures but different sizes, furniture, and equipment deployments. These data are used for model validation in Section III-C.

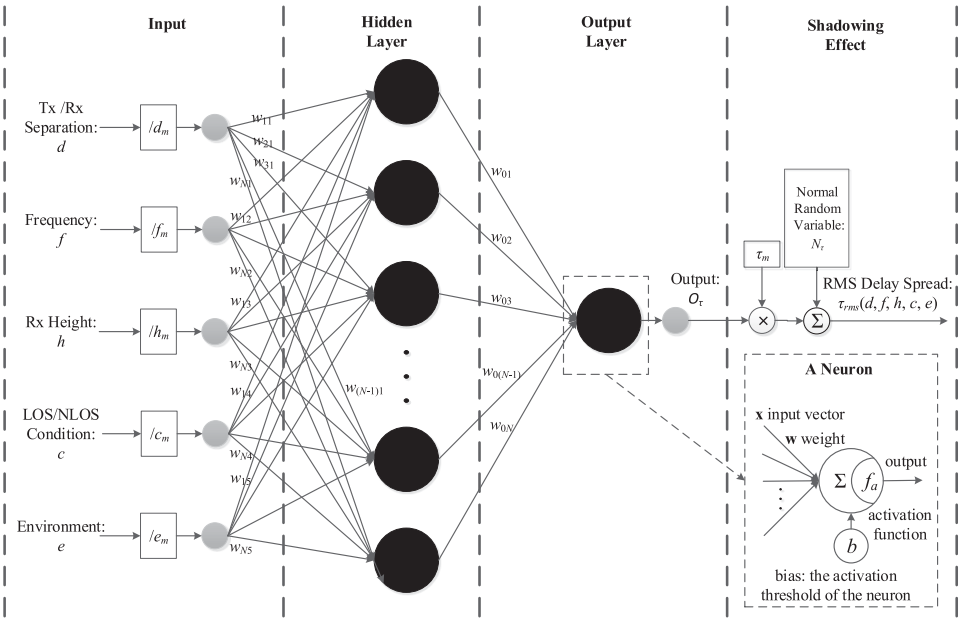

Fig. 2. Proposed neural-network-based RMS delay spread model.

TABLE III
CONFIGURATIONS OF MEASUREMENT SYSTEM

Equipment	Item	Parameters
VNA	Model	Agilent 8720ET
	Measurement frequency	2.5GHz-2.69GHz/4.3GHz-7.3GHz/6GHz-8.5GHz
	Center frequency	2.595GHz/5.8GHz/7.25GHz
	Measurement bandwidth	190MHz/3GHz/2.5GHz
	Transmitting power	10dBm
	Number of sweep point	401
	Sweep time period	400ms
	Noise floor	-110dBm
GPIB	Model	Agilent 82357B
Cable	Tx cable length	5m
	Rx cable length	10m
	cable loss	0.5dB/m
Antenna	Tx type	Omnidirectional monopole
	Rx type	Omnidirectional monopole
	Tx gain	3dBi
	Rx gain	3dBi

B. Measurement System and Data Extraction

The measurement system is a typical vector network analyzer (VNA)-based channel sounder. The detailed illustration of the measurement system can be found in [45]. Its configurations are listed in Table III. Herein, a brief description of the measurement system is given. The VNA sweeps within the measured frequency band (i.e., 2.5–2.69 GHz/4.3–7.3 GHz/6–8.5 GHz) with 10-dBm transmitting power. The Tx and Rx are connected to the port1 and port2 of the VNA, respectively. Then, the S_{21} parameters, corresponding to the frequency response, are captured using this system. The RMS delay spread of the channel can be extracted by the channel impulse responses. The method for extracting the channel parameter is discussed elaborately in [45]. In this article, the RMS delay spread is denoted by $\tau_{rms}(d, f, h, c, e)$, where d is the Tx/Rx separation, f denotes the measured center frequency, h indicates the Rx height, c represents the LOS or NLOS condition, and e means the different indoor environments. The values of c can be $1/0$, denoting LOS and NLOS conditions and the values of e can be $1/2/3$, denoting office, corridor, and stair environments, respectively.

III. NEURAL-NETWORK-BASED RMS DELAY SPREAD MODEL

A. Proposed Model

Theoretically, the RMS delay spread can be divided into two parts [46]. One is the average RMS delay spread, usually described by a determined expression with inputs. The other is the uncertain RMS delay spread, characterized by a random variable. Herein, the two-layer feedforward neural network is used for modeling the determined expression. It has been proved to have high accuracy and good generality when applied to the propagation model [32]–[34]. Meanwhile, the distribution of the random variable is determined to follow normal distribution under the maximum-likelihood estimation (MLE) criterion. Thus, in this article, the RMS delay spread is modeled as a two-layer feedforward neural network plus a normally distributed random variable as illustrated in Fig. 2. As shown in Fig. 2, the black circles in the hidden and output layers are called neurons. They have some computational abilities, such as calculating summation and activation function. Their structures are given in the dashed box of Fig. 2. The activation functions of the hidden and output layers' neurons the are hyperbolic tangent sigmoid (HTS) function as shown in

$$f_a(x) = \frac{1 - e^{-2x}}{1 + e^{-2x}}. \tag{1}$$

The reason for using such functions will be explained in Section III-B. It is seen that there are five inputs, including

the Tx/Rx separation d, frequency f, Rx height h, environment e, and LOS/NLOS condition c. First, the inputs are normalized by their maximum measured values (d_m, f_m, h_m, c_m, and e_m). The normalized inputs (d/d_m, f/f_m, h/h_m, e/e_m, and c/c_m) transmit through the two-layer neural network, and the output (O_τ) can be calculated by

$$O_\tau = f_a\left\{\sum_{j=1}^{N} w_{0j}\left[f_a\left(w_{j1}\frac{d}{d_m}+w_{j2}\frac{f}{f_m}+w_{j3}\frac{h}{h_m}+w_{j4}\frac{c}{c_m}+w_{j5}\frac{e}{e_m}+b_j\right)\right]+b_0\right\}. \tag{2}$$

Then, the average RMS delay spread can be obtained by multiplying the output with the maximum measured RMS delay spread (τ_m), that is $O_\tau \tau_m$. Subsequently, a random variable (N_τ) with normal distribution is added to the average RMS delay spread ($O_\tau \tau_m$). Finally, the RMS delay spread ($\tau_{rms}(d, f, h, c, e)$) can be obtained as

$$\tau_{rms}(d,f,h,c,e) = f_a\left\{\sum_{j=1}^{N} w_{0j}\left[f_a\left(w_{j1}\frac{d}{d_m}+w_{j2}\frac{f}{f_m}+w_{j3}\frac{h}{h_m}+w_{j4}\frac{c}{c_m}+w_{j5}\frac{e}{e_m}+b_j\right)\right]+b_0\right\}\tau_m + N_\tau. \tag{3}$$

It is noteworthy that d, f, h, c, e, and τ_{rms} are all positive values, thus, the normalization values locate in the interval of [0, 1].

In (2) and (3), N is the number of neurons in the hidden layer, $f_a(\cdot)$ is the activation function of the neuron, b_0 is the bias of the neuron in the output layer, w_{0j} ($j = 1, 2, \ldots, N$) is the synaptic weight from the jth hidden layer neuron to the output layer neuron, b_j ($j = 1, 2, \ldots, N$) is the bias of the neuron in the hidden layer, w_{ji} ($j = 1, 2, \ldots, N, i = 1, 2, 3, 4$) is the synaptic weight from the ith input to the jth hidden layer neuron, the order of the inputs is (d, f, h, c, e), N_τ is the shadowing of the RMS delay spread with mean μ_N and standard deviation σ_N, and d_m, h_m, f_m, e_m, c_m, and τ_m are the maximum measured Tx/Rx separation, frequency, Rx antenna height, environment ($e_m = 3$), propagation condition ($c_m = 1$), and RMS delay spread, respectively.

In general, by substituting $f_a(\cdot)$ in (3) with (1), the proposed RMS delay spread model can be descried by (4), shown at the bottom of the page.

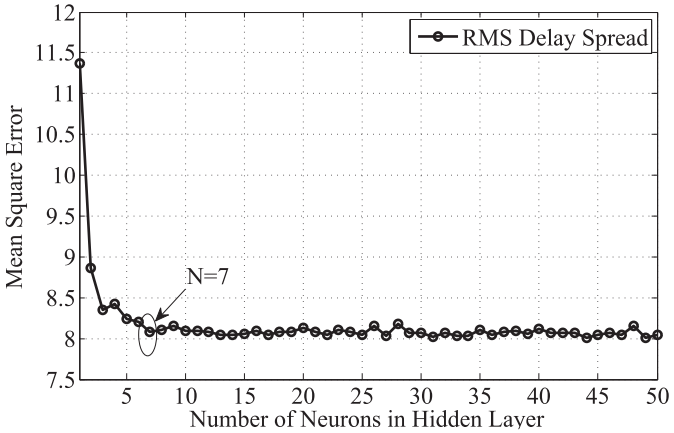

Fig. 3. Number of the neurons versus the MSE.

B. Model Parameters Extraction

It is clearly seen from (4) that the parameters of the proposed models are N, w_{0j}, b_0, w_{ji}, b_j, μ_N, σ_N, d_m, f_m, h_m, c_m, e_m, and τ_m ($i = 1, 2, \ldots, 5, j = 1, 2, \ldots, N$). In addition, the key configurations of the feedforward neural network, including the types of the activation functions in the hidden layer and the output layer, the training methods and weight/bias learning functions, are important for the performance of the model. In this section, these model parameters and neural network configurations should be determined.

First, the number of the neurons in the hidden layer should be extracted. By changing the size of the hidden layer ($N = 1, 2, \ldots, 50$), the mean-square errors (MSEs) between the measured data and the fitted data are calculated. The number of the neurons versus the RMS delay spread is plotted in Fig. 3. As an inspect of Fig. 3, the variation of the MSE becomes small when the number of the neurons is larger than 7. Meanwhile, the computational complexity of the neural network will increase with the number of neurons. Therefore, given the efficiency of the proposed model, N is determined to be 7.

Then, the synaptic weights and the biases of the neural network are trained using the measured data. Usually, in feedforward neural network, the activation functions can be HTS, log sigmoid (LS), and linear (LN) functions, the training method can be Levenberg–Marquardt (LM), scaled conjugate gradient (SCG), gradient descent with momentum and adaptive learning rate (GDX), resilient (RP), and one-step secant (OSS) backpropagation algorithms, and the weight/bias learning function can be gradient descent (GD) and Widrow–Hoff (WH) [43]. The combinations of these configurations (totally $3 \times 3 \times 5 \times 2 = 90$ combinations) are tested, and the MSEs of

$$\tau_{rms}(d,f,h,c,e) = N_\tau + \tau_m \frac{1-e^{-2\left[\sum_{j=1}^{N} w_{0j}\frac{1-e^{-2\left(w_{j1}\frac{d}{d_m}+w_{j2}\frac{f}{f_m}+w_{j3}\frac{h}{h_m}+w_{j4}\frac{c}{c_m}+w_{j5}\frac{e}{e_m}+b_j\right)}}{1+e^{-2\left(w_{j1}\frac{d}{d_m}+w_{j2}\frac{f}{f_m}+w_{j3}\frac{h}{h_m}+w_{j4}\frac{c}{c_m}+w_{j5}\frac{e}{e_m}+b_j\right)}}+b_0\right]}}{1+e^{-2\left[\sum_{j=1}^{N} w_{0j}\frac{1-e^{-2\left(w_{j1}\frac{d}{d_m}+w_{j2}\frac{f}{f_m}+w_{j3}\frac{h}{h_m}+w_{j4}\frac{c}{c_m}+w_{j5}\frac{e}{e_m}+b_j\right)}}{1+e^{-2\left(w_{j1}\frac{d}{d_m}+w_{j2}\frac{f}{f_m}+w_{j3}\frac{h}{h_m}+w_{j4}\frac{c}{c_m}+w_{j5}\frac{e}{e_m}+b_j\right)}}+b_0\right]}} \tag{4}$$

TABLE IV
MSEs OF DIFFERENT CONFIGURATIONS OF THE NEURAL NETWORK

Hidden Layer Activation Function	Output Layer Activation Function	Training Algorithm	Weight/Bias Learning Function	MSE
HTS	**HTS**	**LM**	**GD**	**8.08**
LS	HTS	LM	GD	8.09
LN	HTS	LM	GD	11.36
HTC	LS	LM	GD	35.02
LS	LS	LM	GD	37.14
LN	LS	LM	GD	35.05
HTC	LN	LM	GD	8.16
LS	LN	LM	GD	8.23
LN	LN	LM	GD	11.35
HTS	HTS	SCG	GD	9.75
HTS	HTS	GDX	GD	27.76
HTS	HTS	RP	GD	8.14
HTS	HTS	OSS	GD	9.85
HTS	**HTS**	**LM**	**WH**	**8.08**
HTS	HTS	SCG	WH	9.75
HTS	HTS	GDX	WH	27.76
HTS	HTS	RP	WH	8.14
HTS	HTS	OSS	WH	9.85

TABLE V
EXTRACTED MODEL PARAMETERS

Parameter	Value	Parameter	Value	Parameter	Value
w_{11}	-0.15	w_{51}	1.60	w_{01}	-0.48
w_{12}	1.60	w_{52}	-0.17	w_{02}	0.40
w_{13}	-0.01	w_{53}	0.10	w_{03}	0.09
w_{14}	1.71	w_{54}	0.58	w_{04}	-0.33
w_{15}	0.30	w_{55}	0.21	w_{05}	0.14
w_{21}	-0.35	w_{61}	0.50	w_{06}	1.27
w_{22}	1.49	w_{62}	0.50	w_{07}	-0.23
w_{23}	-0.12	w_{63}	0.13	b_0	-1.96
w_{24}	0.67	w_{64}	-0.14	b_1	-1.46
w_{25}	-1.32	w_{65}	-0.36	b_2	1.27
w_{31}	0.95	w_{71}	0.33	b_3	-0.45
w_{32}	1.52	w_{72}	-2.30	b_4	-1.58
w_{33}	-0.29	w_{73}	0.80	b_5	1.22
w_{34}	0.16	w_{74}	1.34	b_6	1.76
w_{35}	-1.30	w_{75}	-0.43	b_7	-2.71
w_{41}	-0.25	d_m	8.80	μ_X	0
w_{42}	0.42	f_m	7.25	σ_X	2.84
w_{43}	0.19	h_m	1.90	N	7
w_{44}	-0.31	c_m	1	τ_m	33.80
w_{45}	-1.07	e_m	3		

the outputs are compared. A part of them is listed in Table IV. It can be observed that the MSEs of the first line in Table IV are the smallest. That means the combination of the HTS activation functions and the LM backpropagation algorithm works best. In addition, the weight/bias learning function has no impact on the results. Then, such a configuration (first line of Table IV) is used for extracting the model parameters, i.e., w_{0j}, b_0, w_{ji}, and b_j. The MATLAB Neural Network Toolbox is used for training the measured data and generating the simulated data [47]. It is notable that before training the neural network, all the input and output data are normalized using their maximum values for the purpose of the accuracy of the training process. Parameters d_m, f_m, h_m, c_m, e_m, and τ_m are the maximum values of the corresponding input and output of the measured data.

In addition, the shadowing is calculated by subtracting the measured data with the predicted ones (using the same input data) as discussed in [48]. Herein, the concept of the shadowing of the RMS delay spread can be referred to the one of path loss. Then, parameters μ_N and σ_N can be extracted by the MLE method. The probability plots of the shadowing and the normal fit are shown in Fig. 4. It can be seen that the normal random variable matches the shadowing of the RMS delay spread well. The weights and biases of the trained neural network and the other parameters are summarized in Table V.

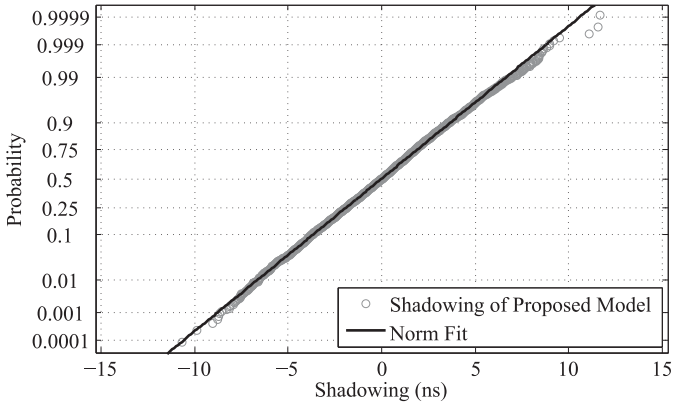

Fig. 4. Probability plots of the shadowing and the normal fit.

C. Model Validation

In this part, the RMS delay spread model used for comparison (called reference model) is the normal distribution random variable model. The proposed model and the reference model are compared and validated using the additional measured data mentioned in Section II. The detailed information about the measured data for model validation is listed in Table VI. In general, the data sets S1–S5 in Table II are used for channel modeling in Sections III-A and III-B, and data sets S6–S15 in Table VI are used for model validation in Section III-C. Herein, the usage of the measured data sets and the process of model validation are briefly illustrated. For the proposed model, the training process is conducted in the phase of model parameters extraction. The configurations in the first line of Table IV are used for training the data sets S1–S5. The LM backpropagation algorithm is used for training. The mean value and standard deviation of shadowing are extracted by MLE. The model parameters can be obtained. Then, the different inputs in data sets S6–S15 are passed through the proposed model with the corresponding model parameters. Finally, the output that is predicted RMS delay spread can be calculated and compared with the measured one. For the reference model, data sets S1–S5 are used for extracting parameters, i.e., the mean value and standard deviation of the normal random variables, by MLE. Then, the RMS delay spread can be generated by such a normal random variable. Finally, the results can be compared with the measured RMS delay spreads.

The RMS delay spreads of the measured data, the proposed model, and the reference model are depicted in Fig. 5. It is observed that the proposed model exhibits the rising trend between the RMS delay spread and the Tx/Rx separation. This is caused by the reason that the LOS components become weak

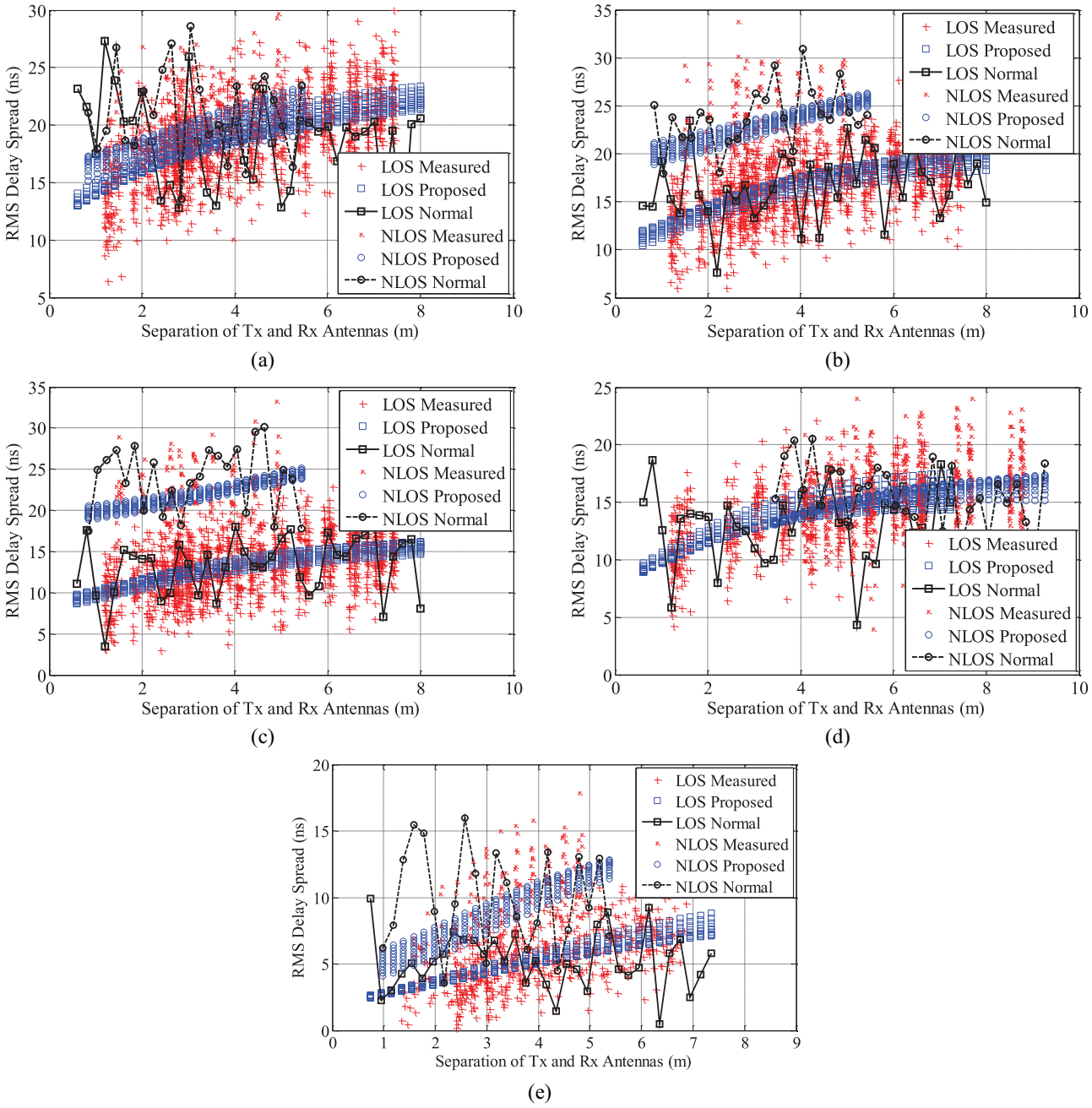

Fig. 5. RMS delay spreads of the measured data, the proposed model, and the normal random variable model: (a) office 2.595 GHz, (b) office 5.8 GHz, (c) office 7.25 GHz, (d) corridor 2.595 GHz, and (e) stair 2.595 GHz.

compared with other components, such as the scatter, reflection, and diffraction ones when the Tx/Rx separation increases, leading to a larger RMS delay spread. Such a tendency is not characterized by the reference model.

In addition, the measured RMS delay spreads scatter around the fitted model (average RMS delay spread). Similar to the shadowing effect of path loss, this phenomenon demonstrates that the shadowing effect exists in the RMS delay spread as well. The more precise of the path loss model, the smaller of shadowing or its standard deviation will be [48]. A similar conclusion can be found in the RMS delay spread model. As shown in Fig. 5, the proposed model is not a line but a surface due to the effect of Rx height. The proposed model covers the measured data better than the log-distance model and its shadowing effect is smaller. This result shows that the proposed model is more precise than the reference model. Moreover, the MSE of the proposed model is 8.08 and one of the normal random variable model is 21.91, verifying the accuracy of the proposed model.

Another advantage of the proposed model is that it has good expansibility and generality. Probably, the distributions of the RMS delay spread will be different under different conditions. In conventional RMS delay spread models, new formulas or complicated correction terms may be imported to the existing models when they are applied to the other environments. In contrast, by taking more extensive measurements

TABLE VI
INFORMATION ABOUT MEASURED DATA USED FOR VALIDATION

Mark	Center Frequency	Environment	Usage	Measured Data Set
S6,S7	2.595GHz	Office	Validation	10 Rx heights 25 Rx points/height 9 grids/point 10 samples/grid total: 22500 samples
S8,S9	2.595GHz	Corridor	Validation	10 Rx heights 20 Rx points/height 9 grids/point 10 samples/grid total: 18000 samples
S10,S11	2.595GHz	Stair	Validation	10 Rx heights 20 Rx points/height 5 grids/point 10 samples/grid total: 10000 samples
S12,S13	5.8GHz	Office	Validation	10 Rx heights 25 Rx points/height 9 grids/point 10 samples/grid total: 22500 samples
S14,S15	7.25GHz	Office	Validation	10 Rx heights 25 Rx points/height 9 grids/point 10 samples/grid total: 22500 samples

and retraining the neural network, the proposed model can be extended to different environments without changing the structure of the model. Additionally, more important inputs, such as the Tx antenna height, the antenna type, etc., can be imported to the proposed model by increasing the number of inputs and adjusting the number of the neurons. The proposed model can also be extended to describe the dynamic channels. Herein, the process is illustrated. First, the measurement system in the time domain, such as the direct RF pulse measurement system and spread spectrum sliding correlator channel sounder, should be adopted to capture the fast fading dynamic channel data [12], [49], or the open data of dynamic channels obtained by other researchers could be used [50]. The data related to the users' motion or users' density should be recorded as well. Second, based on the proposed model, the inputs, including the speed of motion, the direction of motion, and the number of users and time are added to the neural network. Then, the measured input and output data are used to extract the model parameters according to the process in Section III-B. Finally, the proposed model describing the users' motion and users' density can be obtained. Thus, a more general RMS delay spread model suitable for more complex and ubiquitous IoTs scenarios can be easily obtained under such a neural network-based framework.

IV. CONCLUSION

The RMS delay spread is modeled as a generalized two-layer feedforward neural network plus a random variable. The framework of the neural network-based RMS delay spread model is discussed at first. In the proposed model, its dependencies on the Tx/Rx separation, frequency, antenna height, environment, and LOS/NLOS condition are characterized. Moreover, the shadowing effect describing the uncertainty of the RMS delay spread is modeled by a normal random variable. In addition, the effects of the neural network configurations on the accuracy of the proposed model are researched. It is found that the combination of HTS activation functions and the LM backpropagation algorithm is the best configuration of the neural network. The proposed model is experimentally validated as well. Compared with the normal random variable RMS delay spread model, the proposed model contains more information about the environments, thus, exhibiting higher accuracy. Additionally, it can be easily extended to other scenarios by including more inputs, adjusting the number of neurons and retraining the neural network without introducing any correction term or changing the basic framework of the proposed model. The proposed model is expected to provide significant information for network planning, system design, and performance improvement in future ubiquitous IoTs scenarios.

ACKNOWLEDGMENT

The authors would like to thank Y. Chen, X.-T. Wu, Z. Ma, B.-L. Jian, Dr. P.-F. Cui, Dr. J. She, Dr. Y. Wang, Q. Yan, X.-L. Wang, B. Yang, and other members of Nanjing University of Posts and Telecommunications and China Telecommunication Technology Labs for their assistance in the channel measurement. They are also indebted to the anonymous reviewers for their beneficial comments on this article.

REFERENCES

[1] P. Demestichas *et al.*, "5G on the horizon: Key challenges for the radio-access network," *IEEE Veh. Technol. Mag.*, vol. 8, no. 3, pp. 47–53, Sep. 2013.
[2] A. Yang, X. Yang, J. Chang, B. Bai, F. Kong, and Q. Ran, "Research on a fusion scheme of cellular network and wireless sensor for cyber physical social systems," *IEEE Access*, vol. 6, pp. 18786–18794, 2018.
[3] D. Minoli, K. Sohraby, and B. Occhiogrosso, "IoT considerations, requirements, and architectures for smart buildings—Energy optimization and next-generation building management systems," *IEEE Internet Things J.*, vol. 4, no. 1, pp. 269–283, Feb. 2017.
[4] J. Lin, W. Yu, N. Zhang, X. Yang, H. Zhang, and W. Zhao, "A survey on Internet of Things: Architecture, enabling technologies, security and privacy, and applications," *IEEE Internet Things J.*, vol. 4, no. 5, pp. 1125–1142, Oct. 2017.
[5] W. Xu *et al.*, "The design, implementation, and deployment of a smart lighting system for smart buildings," *IEEE Internet Things J.*, vol. 6, no. 4, pp. 7266–7281, Aug. 2019.
[6] C. Brooks *et al.*, "A component architecture for the Internet of Things," *Proc. IEEE*, vol. 106, no. 9, pp. 1527–1542, Sep. 2018.
[7] A. Burg, A. Chattopadhyay, and K.-Y. Lam, "Wireless communication and security issues for cyber-physical systems and the Internet-of-Things," *Proc. IEEE*, vol. 106, no. 1, pp. 38–60, Jan. 2018.
[8] Z. Ma, M. Xiao, Y. Xiao, Z. Pang, H. V. Poor, and B. Vucetic, "High-reliability and low-latency wireless communication for Internet of Things: Challenges, fundamentals, and enabling technologies," *IEEE Internet Things J.*, vol. 6, no. 5, pp. 7946–7970, Oct. 2019.
[9] J. G. Proakis and M. Salehi, *Digital Communications*. New York, NY, USA: McGraw-Hill, 2007, p. 384.
[10] A. Asp, S. F. Yunas, V. Kilpelaeinen, J. Niemelae, and M. Valkama, "Passive intermodulation and network planning challenges in future indoor networks and energy efficient buildings," in *Proc. Eur. Wireless Conf.*, Oulu, Finland, 2016, pp. 1–7.
[11] S. Bera and S. K. Subir, "Review on indoor channel characterization for future generation wireless communications," in *Proc. Adv. Commun. Devices Netw.*, vol. 537, 2018, pp. 349–356.
[12] T. S. Rappaport, *Wireless Communications: Principles and Practice*. Upper Saddle River, NJ, USA: Prentice-Hall, 2002.

[13] Q. Shi and Y. Luo, "Low-complexity RMS delay spread estimation for wireless OFDM systems," in *Proc. IEEE Int. Conf. Commun. Technol.*, 2017, pp. 1397–1401.
[14] J. T. E. McDonnell, T. P. Spiller, and T. A. Wilkinson, "Characterization of the spatial distribution of RMS delay spread in indoor LOS wireless environments at 5.2 GHz," in *Proc. IEEE Int. Symp. Pers. Indoor Mobile Radio Commun.*, vol. 2. Boston, MA, USA, 1998, pp. 621–624.
[15] M. S. Varela and M. G. Sanchez, "RMS delay and coherence bandwidth measurements in indoor radio channels in the UHF band," *IEEE Trans. Veh. Technol.*, vol. 50, no. 2, pp. 515–525, Mar. 2001.
[16] Y. Wang, W. Lu, and H. Zhu, "Experimental study on indoor channel model for wireless sensor networks and Internet of Things," in *Proc. IEEE Int. Conf. Commun. Technol.*, Nanjing, China, 2010, pp. 624–627.
[17] Z. Jiang, J. Yu, R. Zhu, K. Yang, and W. Chen, "Experimental multipath delay spread and path loss analysis for the indoor environment at 5.9 GHz," in *Proc. Int. Conf. Wireless Commun. Signal Process. Netw.*, Chennai, India, 2016, pp. 1859–1863.
[18] M. K. Awad, K. T. Wong, and Z. Li, "An integrated overview of the open literature's empirical data on the indoor radiowave channel's delay properties," *IEEE Trans. Antennas Propag.*, vol. 56, no. 5, pp. 1451–1468, May 2008.
[19] H. Hashemi and D. Tholl, "Analysis of the RMS delay spread of indoor radio propagation channels," in *Proc. Int. Conf. Commun.*, vol. 2. Chicago, IL, USA, 1992, pp. 875–881.
[20] S. Tanchotikul, P. Supanakoon, S. Promwong, and J. Takada, "Statistical model RMS delay spread in UWB ground reflection channel based on peak power loss," in *Proc. Int. Symp. Commun. Inf. Technol.*, 2006, pp. 619–622.
[21] E. Zöchmann *et al.*, "Directional evaluation of receive power, Rician K-factor and RMS delay spread obtained from power measurements of 60 GHz indoor channels," in *Proc. IEEE-APS Topical Conf. Antennas Propag. Wireless Commun.*, 2016, pp. 246–249.
[22] J. Li, B. Ai, R. He, M. Yang, and Z. Zhong, "Multi-frequency channel characterization for massive MIMO communications in lobby environment," *China Commun.*, vol. 16, no. 9, pp. 79–92, Sep. 2019.
[23] J. Pan and J. McElhannon, "Future edge cloud and edge computing for Internet of Things applications," *IEEE Internet Things J.*, vol. 5, no. 1, pp. 439–449, Feb. 2018.
[24] J. Park, S. Samarakoon, M. Bennis, and M. Debbah, "Wireless network intelligence at the edge," *Proc. IEEE*, vol. 107, no. 11, pp. 2204–2239, Nov. 2019.
[25] E. D. Ayele, C. Hakkenberg, J. P. Meijers, K. Zhang, N. Meratnia, and P. J. M. Havinga, "Performance analysis of LoRa radio for an indoor IoT applications," in *Proc. Int. Conf. Internet Things Global Community*, 2017, pp. 1–8.
[26] Y. Wang, Ye, W. J. Lu, and H. B. Zhu, "An empirical path-loss model for wireless channels in indoor short-range office environment," *Int. J. Antennas Propag.*, vol. 2012, p. 7, Feb. 2012.
[27] A. Horch, M. Kubach, H. Roßnagel, and U. Laufs, "Why should only your home be smart? A vision for the office of tomorrow," in *Proc. IEEE Int. Conf. Smart Cloud*, New York, NY, USA, 2017, pp. 52–59.
[28] P. S. Hall, M. Ricci, and T. M. Hee, "Measurements of on-body propagation characteristics," in *Proc. IEEE Int. Symp. Antennas Propag. Soc.*, vol. 2. San Antonio, TX, USA, 2002, pp. 310–313.
[29] M. M. Khan, Q. H. Abbasi, A. Alomainy, and Y. Hao, "Radio propagation channel characterisation using ultra wideband wireless tags for body-centric wireless networks in indoor environment," in *Proc. Int. Workshop Antenna Technol.*, Hong Kong, 2011, pp. 202–205.
[30] P. J. Y. Piera and J. K. G. Salva, "A wireless sensor network for fire detection and alarm system," in *Proc. Int. Conf. Inf. Commun. Technol.*, Kuala Lumpur, Malaysia, 2019, pp. 1–5.
[31] T. Beibei and L. Yi, "Upgraded application of intelligent environment monitoring system in IOT smart home," in *Proc. Int. Conf. Intell. Syst. Design Eng. Appl.*, 2015, pp. 916–919.
[32] S. M. Aldossari and K. C. Chen, "Machine learning for wireless communication channel modeling: An overview," *Wireless Pers. Commun.*, vol. 106, no. 1, pp. 41–70, 2019.
[33] A. Massa, D. Marcantonio, X. Chen, M. Li, and M. Salucci, "DNNs as applied to electromagnetics, antennas, and propagation—A review," *IEEE Antennas Wireless Propag. Lett.*, vol. 18, no. 11, pp. 2225–2229, Nov. 2019.
[34] W. Jiang and H. D. Schotten, "Neural network-based fading channel prediction: A comprehensive overview," *IEEE Access*, vol. 7, pp. 118112–118124, 2019.
[35] I. Popescu, I. Nafomita, P. Constantinou, A. Kanatas, and N. Moraitis, "Neural networks applications for the prediction of propagation path loss in urban environments," in *Proc. IEEE Veh. Technol. Conf.*, vol. 1. Rhodes, Greece, 2001, pp. 387–391.
[36] M. Kalakh, N. Kandil, and N. Hakem, "Neural networks model of an UWB channel path loss in a mine environment," in *Proc. IEEE Veh. Technol. Conf. (VTC Spring)*, 2012, pp. 1–5.
[37] J. C. D. Cruz and F. S. Caluyo, "Heuristic modelling of path loss inside residences at 677MHz," in *Proc. Int. Conf. Humanoid Nanotechnol. Inf. Technol. Commun. Control Environ Manag.*, 2014, pp. 1–5.
[38] T. A. Benmus, R. Abboud, and M. K. Shatter, "Neural network approach to model the propagation path loss for great Tripoli area at 900, 1800, and 2100 MHz bands," in *Proc. Int. Conf. Sci. Techn. Autom. Control Comput. Eng.*, 2015, pp. 793–798.
[39] M. Kotol and Z. Raida, "Comparison of neural models of UWB and 60GHz in-car transmission channels," in *Proc. Int. Conf. Broadband Commun. Next Gener. Netw. Multimedia Appl.*, 2016, pp. 1–4.
[40] A. Bhuvaneshwari, R. Hemalatha, and T. Satyasavithri, "Performance evaluation of dynamic neural networks for mobile radio path loss prediction," in *Proc. IEEE Uttar Pradesh Int. Conf. Elect. Comput. Electron. Eng.*, 2016, pp. 461–466.
[41] H. A. O. Cruz, R. N. A. Nascimento, J. P. L. Araujo, E. G. Pelaes, and G. P. S. Cavalcante, "Methodologies for path loss prediction in LTE-1.8 GHz networks using neuro-fuzzy and ANN," in *Proc. Int. Microw. Optoelectron. Conf.*, 2017, pp. 1–5.
[42] S. P. Sotiroudis, S. K. Goudos, and K. Siakavara, "Neural networks and random forests: A comparison regarding prediction of propagation path loss for NB-IoT networks," in *Proc. Int. Conf. Modern Circuits Syst. Technol.*, Thessaloniki, Greece, 2019, pp. 1–4.
[43] S. I. Popoola *et al.*, "Determination of neural network parameters for path loss prediction in very high frequency wireless channel," *IEEE Access*, vol. 7, pp. 150462–150483, 2019.
[44] A. Asp, Y. Sydorov, M. Keskikastari, M. Valkama, and J. Niemela, "Impact of modern construction materials on radio signal propagation: Practical measurements and network planning aspects," in *Proc. IEEE Veh. Technol. Conf.*, Seoul, South Korea, 2014, pp. 1–7.
[45] Y. Yu, Y. Liu, W. Lu, and H. Zhu, "Measurement and empirical modelling of root mean square delay spread in indoor femtocells scenarios," *IET Commun.*, vol. 11, no. 13, pp. 2125–2131, 2017.
[46] G. Xiaotao, H. Zhao, Z. Yichi, Z. Xin, and N. Meining, "Theoretical uncertainty of RMS delay spread simulated by reverberation chamber," in *Proc. IEEE Int. Conf. Electron. Meas. Instrum.*, 2015, pp. 426–430.
[47] (2019). *MATLAB NFTOOL*. [Online]. Available: https://ww2.mathworks.cn/help/deeplearning/ref/nftool.html
[48] Y. Yu, Y. Liu, W.-J. Lu, and H.-B. Zhu, "Path loss model with antenna height dependency under indoor stair environment," *Int. J. Antennas Propag.*, vol. 2014, p. 6, Jul. 2014.
[49] D. Tholl, M. Fattouche, R. J. C. Builtitude, P. Melancon, and H. Zaghloul, "A comparison of two radio propagation channel impulse response determination techniques," *IEEE Trans. Antennas Propag.*, vol. 41, no. 4, pp. 515–517, Apr. 1993.
[50] Y. Wang, W.-J. Lu, and H.-B. Zhu, "Propagation characteristics of the LTE indoor radio channel with persons at 2.6 GHz," *IEEE Antennas Wireless Propag. Lett.*, vol. 12, pp. 991–994, 2013.

Yu Yu was born in Nanjing, China, in 1990. He received the B.E. and Ph.D. degrees in communication and information system from Nanjing University of Posts and Telecommunications, Nanjing, in 2012 and 2017, respectively.

He was a Research Engineer with Huawei Technologies Company, Ltd, Shenzhen, China. He is currently a Lecturer with the School of Information and Communication Engineering, Nanjing Institute of Technology, Nanjing. He has authored and coauthored over ten technical papers published in peer-reviewed international journals and conference proceedings. His research interests include wireless propagation and wireless channel modeling.

Wen-Jun Lu (Senior Member, IEEE) received the Ph.D. degree in electronic engineering from Nanjing University of Posts and Telecommunications (NUPT), Nanjing, China, in 2007.

He has been a Professor with Jiangsu Key Laboratory of Wireless Communications, NUPT, since 2013. He has authored or coauthored over 180 technical papers published in peer-reviewed international journals and conference proceedings. He is the translator of the Chinese version the *Art and Science of Ultrawideband Antennas* (by H. Schantz). He has authored the book *Antennas: Concise Theory, Design and Applications* (in Chinese). His research interests include antenna theory, antenna/array designs, wireless propagation, and channel modeling.

Prof. Lu was a recipient of the Exceptional Reviewers Award of the IEEE TRANSACTIONS ON ANTENNAS AND PROPAGATION in 2016. He has been serving as an Editorial Board Member for the *International Journal of RF and Microwave Computer-Aided Engineering* since 2014. He has been serving as an Associate Editor for *Electronics Letters* since 2019.

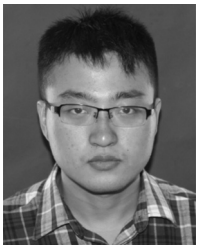

Yang Liu (Member, IEEE) was born in Wuxi, China, in 1988. He received the Ph.D. degree in communication and information system from the Key Laboratory of Wireless Communication, Nanjing University of Posts and Telecommunications, Nanjing, China, in 2016.

He is currently a Lecturer with the Institute of IOT Engineering, Jiangnan University, Wuxi. He has authored and coauthored over ten technical papers published in peer-reviewed international journals and conference proceedings. His research interests include the wireless propagation and wireless channel modeling.

Hong-Bo Zhu was born in Yangzhou, China, in 1956. He received the Ph.D. degree in telecommunication engineering from Beijing University of Posts and Telecommunications, Beijing, China, in 1996.

He is currently the Standing Director of the Chinese Institute of Electronics, Beijing, China, and the Director of Jiangsu Key Laboratory of Wireless Communications, Nanjing University of Posts and Telecommunications, Nanjing, China. He has authored and coauthored over 100 journal papers and over 60 invention patents authorized. In the past five years, he has undertaken over 30 projects at the national, provincial, and ministerial level. His research interests include wireless communications, Internet of Things, and EMC.